Available online at www.elixirpublishers.com (Elixir International Journal)

Vibrational Spectroscopy

Elixir Vib. Spec. 92 (2016) 38798-38804

ISSN: 2229-712X

Vibrational Spectroscopic, NBO, Homo-Lumo and First-Order Hyperpolarizability Analyses of 2,4-Dichloro-Alpha, Alpha, Alpha Trifluorotoluene By Density Functional Method

P.Chitradevi[1], M. Arivazhagan[2] and S. Manivel[2]

[1]Research Department of Physics, Rajah Serfoji Govternment College,Thanjavur-613005, TN, India.

[2]Research Department of Physics, Government Arts College, Trichy 22, TN, India.

ARTICLE INFO

Article history:

Received: 8 October 2015;

Received in revised form:

1 March 2016;

Accepted: 4 March 2016;

Keywords

FTIR,

FT-Raman,

DFT Calculations,

Dichloro-A,A,A-Trifluorotoluene.

ABSTRACT

The FT-IR and FT-Raman spectra of 2,4-dichloro-α,α,α-trifluorotoluene (DαααTFT) have been recorded in the range of 4000–400 cm^{-1} and 3500–50 cm^{-1} respectively. The molecular geometry and vibrational frequencies in the ground state are calculated using the LSDA and B3LYP method with 6-311+G(d, p) and 6-311++G (d, p) basis sets . The computed values of frequencies are scaled using a suitable scale factor to yield good coherence with the observed values. Most of the modes have wave numbers in the expected range. The calculated HOMO–LUMO energy gap shows that charge transfer occur within the molecule. NBO analysis has been performed in order to elucidate charge transfers or conjugative interaction, the intra-molecule hybridization and delocalization of electron density within the molecule. The total energy distribution (TED) has also been calculated for each mode of the vibration of the molecule.

Introduction

Derivatives of dichloro-α,α,α-trifluorotoluene (DαααTFT) have got wide applications, such as anti-bacterial agents, central nervous system depressants, tranquilizers for alleviation of anxiety, anti-malarial agent-mefloquine, for heat transfer printing of Polyester textiles, insecticides, a developer (blue) for use in sensitive diazo process mutagenic activity, intermediate for dyes, germicides, pharmaceuticals, crop protectants, intermediates for dye, colourant manufacture and fungicide [1-9]. dichloro-α,α,α-trifluorotoluene (DαααTFT) is very important due to its extensive use as intermediate for pharmaceutical [10]. Fluoride alters the maturation process of the enamel and reacts with its structure to form fluorapatite, which is more stable and more resistant to acid corrosion than hydroxypatite [11,12]. This is the principle of the topical application or systemic use of fluoride, which prevents and diminishes the risk of dental cares. However, excess fluoride during enamel formation, particularly during the maturation phase of amelogenesis, causes both esthetic and functional defects in teeth [13].

Consideration of these factors leads to undertake the detailed spectral investigation of 2,4-dichloro-α,α,α-trifluorotoluene (DαααTFT). Optimized geometries of the molecule have been interpreted and compared with the reported experimental values. The experimental geometrical parameters show satisfactory agreement with the theoretical prediction from DFT. The scaled vibrational frequencies at LSDA/B3LYP/6-311++G(d,p) seem to coincide with the experimentally observed values with acceptable deviations. In particular, for polyatomic molecules the DFT methods lead to the prediction of more accurate molecular structure and vibrational frequencies. In DFT methods, local-spin density approximation LSDA [14-17] generally gives good molecular structures, vibrational frequencies, charges and densities in strongly bounded systems, Becke's three parameter hybrids function combined with the Lee-Yang-Parr correlation function (B3LYP) [18-19] predict the best results for molecular geometry and vibrational wave numbers for moderately larger molecule.

Experimental Details

The FT-IR spectrum of the DαααTFT molecule is recorded in BRUKER IFS 66 V spectrometer in the range of 4000 - 400 cm^{-1}. The spectral resolution is ± 2 cm^{-1}. Additional supports for the vibrational assignments are obtained from the FT-Raman spectrum. So the FT-Raman spectrum of this molecule is also recorded with FRA 106 Raman module equipped with Nd:YAG laser source operating at 1.064 µm line widths with 200 mw power. The spectrum was recorded in the range of 3500 - 50 cm^{-1} with scanning speed of 30 cm^{-1} min^{-1} of spectral width 2 cm^{-1}. The frequencies of all sharp bands are accurate to ± 1 cm^{-1}.

Computational Methods

The molecular structure of DαααTFT in the ground state is computed by performing DFT (LSDA and B3LYP) with 6-311++G(d,p) basis set using GAUSSIAN 09W program [20]. Structural parameters are used in the vibrational frequency calculations in DFT method. Geometries have been first optimized with full relaxation on the potential energy surfaces at LSDA/6-311++G(d,p) basis set. The optimized geometrical parameters, fundamental vibrational frequencies, IR and Raman intensities are calculated using the GAUSSIAN 09W package program.

By combining the results of the GAUSSVIEW [21]program with symmetry considerations, vibrational frequency assignments are made with a high degree of accuracy. There may be some mismatch in defining internal co-ordination. But the defined co-ordinate forms complete set and matches quite well with the motions observed using GASSVIEW program.

Tele:

E-mail address: jjmarivu@yahoo.co.in

Results and Discussion

Molecular Geometry

The optimized molecular structure of DαααTFT is shown in Fig. 1.

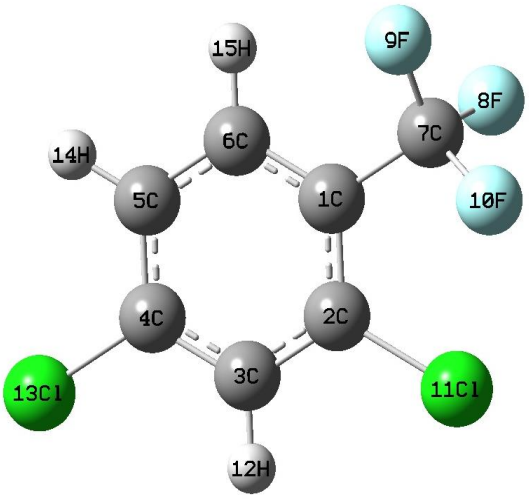

Fig 1.Optimized molecular structure of 2,4-dichloro-ααα-trifluorotoluene

The global minimum energy is obtained by DFT structure optimization based on LSDA/6-311++G(d,p),B3LYP/6-311++G(d,p) basis set for DαααTFT as -1483.358723 and -1488.529710 Hartrees, respectively. The comparative optimized structural parameters such as bond lengths, bond angles and dihedral angles are presented in Table 1.

From the theoretical values, it is found that most of the optimized bond lengths are slightly larger than the experimental values, due to that the theoretical calculations of isolated molecules in gaseous phase and the experimental results of molecules are in solid state. Comparing bond angles and lengths of LSDA/B3LYP, the values of the B3LYP method are larger.

According to the computed values B3LYP/6-311++G(d,p), the entire C-C bond lengths of the benzene ring differ from one another by 0.001A° to 0.004A°. Hence the hexagonal structure of the benzene ring is not affected by a large amount due to the CCl and CH substitutions. The experimental bond length of C-Cl is 1.781 A° and 1.774 A° [22] and they nearly coincides with the calculated value from LSDA/6-311++G(d,p) method. The bond lengths of C–H calculated by DFT with LSDA/B3LYP/6-311++G(d,p) are 1.475 A° and 1.496 A°, respectively. On comparing these values with experimental value of 1.469 A°, it is seen that the DFT (LSDA/B3LYP) overestimates the bond length. Another value of C-C bond length of LSDA/6-311++G(d,p) is 1.089 A°. The bond lengths of C-F calculated by DFT with LSDA/B3LYP/6-311++G(d,p) are 1.387 A° and 1.401 A° respectively, while comparing these values with experimental value of 1.375 A°, the symmetry of the benzene ring is not disturbed to a great extent and is evident by the CCC bond angle C1-C2-C3 ≈ C3-C4-C5 ≈ C4-C5-C6 ≈ 121°, C4-C3-C2 ≈ C6-C1-C2 ≈ 118°, C4-C5-C6 ≈ 120°. The value of the bond angle CCCl bond angle is C3-C4-Cl13 ≈ C5-C4-Cl13 ≈ 119°. The value of the bond angle C4-C5-H14 (~ 121.1°) calculated by LSDA/B3LYP/ 6-311++G(d,p) is 1.1° higher than the experimental value of 120° whereas the value of the bond angle is C6-C5-C4 ≈ C1-C6-H15 ≈ C5-C6 ≈ H15 ≈ 120°. The value of the bond angle F9-C7-F8 ≈ F9-C7-F10 ≈ F8-C7-F10 ≈ 106° is calculated by LSDA/B3LYP/6-311++G(d,p) methods.

Vibrational Assignments

The DαααTFT consists of 15 atoms, and belongs to C_1 point group symmetry. Hence the number of normal modes of vibrations for DαααTFT works to 39. The observed FTIR and FT-Raman spectra of DαααTFT are shown in Fig.2 and 3, respectively.

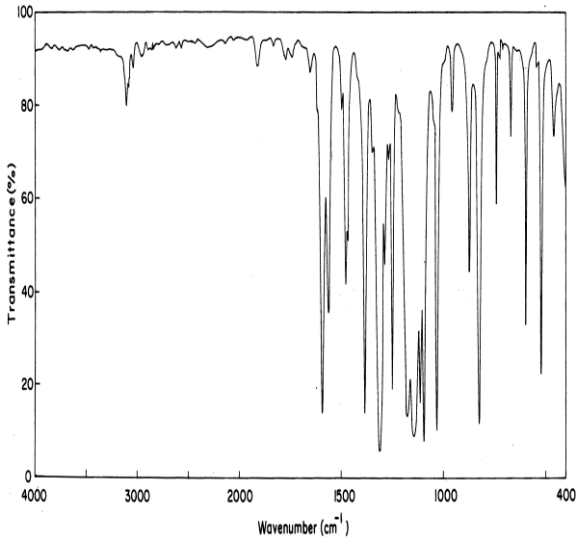

Fig 2. FT-IR spectrum of 2,4-dichloro-ααα-trifluorotoluene

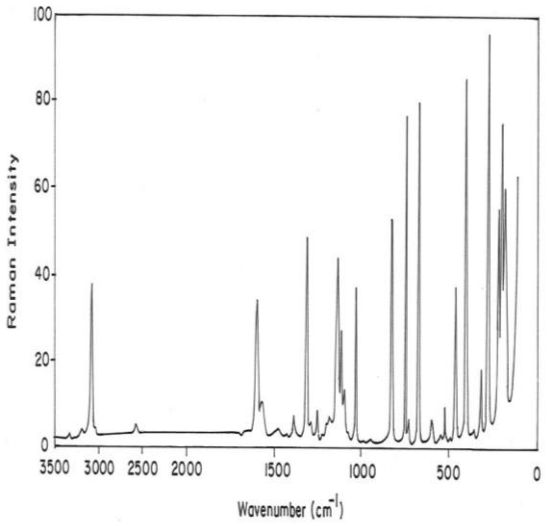

Fig 3. FT-Raman spectrum of 2,4-dichloro-ααα-trifluorotoluene

The harmonic vibrational frequencies calculated for DαααTFT at DFT–LSDA/B3LYP levels using 6-311++G(d,p) basis set, observed FTIR and FT-Raman frequencies for various modes of vibrations are presented in Table 2.

C-H Vibrations

The aromatic organic compounds structure shows the presence of asymmetric C-H stretching vibrations in the region 3100 - 3000 cm^{-1} [23,24]. This is the characteristic region for recognition on C-H stretching vibrations. In the present investigation, the bands observed at 3111, 3099 cm^{-1} in FT-IR and 3095 cm^{-1} in FT-Raman spectra have been assigned to C-H stretching vibrations for DαααTFT. The C-H in-plane and out-of-plane bending vibrations normally take place as a number of strong to weak intensity sharp bands in the region of 1300 - 1000 cm^{-1} and 1000 - 750 cm^{-1} [25-31], respectively. The bands for C-H in-plane bending vibrations are identified at 1180, 1148 and 1108 cm^{-1} in FTIR and the C-H out-of-plane bending vibrations are found at 963, 871 and 819 cm^{-1} in FTIR spectrum for DαααTFT.

C=C and C-C Vibrations

The six ring carbon atoms undergo coupled vibrations which are known as skeletal vibrations given a maximum of

three bands in the region 1660 - 1420 cm^{-1}. As predicted in the earlier references [32], the prominent peaks at 1600, 1576 and 1568 cm^{-1} in FTIR spectrum are due to strong C=C stretching vibrations and 1390, 1332, 1295 cm^{-1} in FTIR spectrum and 1319 cm^{-1} in FT-Raman spectrum are due to strong, C-C skeletal vibrations for the title compound. These peaks confirm that the compound is aromatic in nature [33] The peak is assigned at 733 cm^{-1} in FTIR spectrum and 409 cm^{-1} in FT-Raman spectrum due to C-C in-plane bending vibrations and out-of-plane bending vibrations respectively. Except C-C vibration, all the C=C stretching vibrations are coherent with the literature data [34].

C-Cl Vibrations

The C-Cl stretching band is normally expected around 750–580 cm^{-1} [35] Strong FT-Raman bands are assigned at 748 and 679 cm^{-1} due to C-Cl stretching vibrations. The C-Cl deformation vibrations are expected around 460–175 cm^{-1} [36]. The peaks are assigned at 323 and 282 cm^{-1} in FT-Raman spectrum due to C-Cl in-plane bending vibrations, and FT-Raman bands at 218 and 205 cm^{-1} are assigned to the C-Cl out-of-plane bending vibrations, when comparison is made with the assignments given in literature [37]

CF_3 Vibrations

Usually symmetric and antisymmetric CF_3 stretching vibrations are in the region 1290 - 1235 and 1226 - 1200 cm^{-1} respectively [38-39] Therefore the bands located at 1273 cm^{-1} in FTIR spectrum and 1230 cm^{-1} in FT-Raman spectrum are assigned to symmetric and antisymmetric stretching vibrations. C-F deformations usually occur in regions 690 - 631 cm^{-1}, 640 - 580 cm^{-1} and 570 - 510 cm^{-1} [24] Accordingly CF_3 sb, CF_3 ipb and CF_3 opb are identified at 667, 603 and 528 cm^{-1} in FT-Raman spectrum respectively. They also supported by the literature [40,41]. CF_3 rocking vibrational frequency ranges at 460–350 cm^{-1}. In the present investigation, the bands located at 457 cm^{-1} in FTIR spectrum and 351 cm^{-1} in FT-Raman spectrum are assigned to rocking modes of CF_3 ipr and CF_3 opr respectively. CF_3 out-of-plane stretching and twisting modes are also identified and listed in Table 2.

NBO Study

In NBO analysis large $E^{(2)}$ value shows the intensive interaction between electron donors and electron-acceptors and greater the extent of conjugation of the whole system, the possible intensive interactions are given in Table 3. The second-order perturbation theory analysis of Fock matrix in NBO basis shows intramolecular hyper conjugative interactions of π electrons [42] A filled bonding or lone pair orbital can act as a donor and an empty or filled bonding, anti bonding or lone pair orbital can act as an acceptor. These interactions can strengthen and weaken the bonds. For example, a lone pair donor-anti bonding acceptor orbital interaction will weaken the bond associated with anti bonding orbital. Conversely, an interaction with a bonding pair as the acceptor will strengthen the bond. Strong electron delocalization in Lewis structure will also show up as donor-acceptor interaction.

For each donor (i) and acceptor (j), the stabilization energy $E^{(2)}$ associates with the delocalization $i \rightarrow j$ is estimated as

$$E^{(2)} = \Delta E_{ij} = q_i \frac{F(i,j)^2}{\varepsilon_j - \varepsilon_i} \qquad (1)$$

Where q_i is the donor orbital occupancy ε_j and ε_i are diagonal elements orbital energies and F(i,j) is the off diagonal NBO Fock matrix element. Larger $E^{(2)}$ value, the more intensive is the interaction between electron donors and acceptors i.e., the more donation tendency from electron donors to electron acceptor and greater the extent of conjugation of the whole system [43]. Delocalization of electron density between occupied Lewis type (bond or lone pair) NBO orbital and formally unoccupied (antibond or Rydberg) non-Lewis NBO orbital corresponds to a stabilizing donor-acceptor interaction.

NBO analysis has been performed on the title molecule at the DFT/B3LYP level in order to elucidate charge transfers or conjugative interaction, the intra-molecular rehybridization and delocalization of electron density within the molecule. The second order perturbation theory analysis of Fock matrix in the NBO basis of the molecule shows the strong intra molecular hyper conjugative interactions which are presented in the Table 3. The intramolecular hyper conjugative interactions are formed by the orbital overlap between n_3(Cl) and σ^*(C-C) bond orbital which results in ICT (intra molecular charge transfer) causing stabilization of the system. n-π conjucation between the F and Cl lone pair electrons and benzene ring π system is strong in the ground state. n_3(F8) $\rightarrow$ σ^*(C7-F9), n_3(F10) $\rightarrow$ σ^*(C7-F9), n_3(Cl11) $\rightarrow$ π^*(C1-C2), n_3(Cl13) $\rightarrow$ π^*(C3-C4) energies are 5.99, 5.97, 7.06, 6.63 kJ mol^{-1} respectively shows n-π-conjugation between fluorine, chlorine and benzene ring. In DαααTFT π^*(C1-C2) $\rightarrow$ π^*(C5-C6) and π^*(C3-C4) $\rightarrow$ π^*(C5-C6), these interactions are seen to give a strong stabilizations 80.72 and 81.83 kJ mol^{-1} respectively. This strong stabilization denotes the larger delocalization. Hence this structure is stabilized by these orbital interactions.

Homo-Lumo Analysis

Many organic molecules, containing conjugated π electrons are characterized by large values of molecular first-order hyperpolarizabilities, and are analyzed by means of vibrational spectroscopy [44,45] The analysis of the wave function indicated that the electronic absorption corresponds to the transition from the ground to the first excited state and is mainly described by one electron excitation from the highest occupied molecular orbital (HOMO) to the lowest unoccupied molecular orbital (LUMO) [46,47]

The HOMO is located over Benzene ring, chlorine group consecutively the HOMO-LUMO transition implies an electron density transfer to the fluoro group from benzene ring, chlorine, hydrogen group and that is shown in Fig 4.

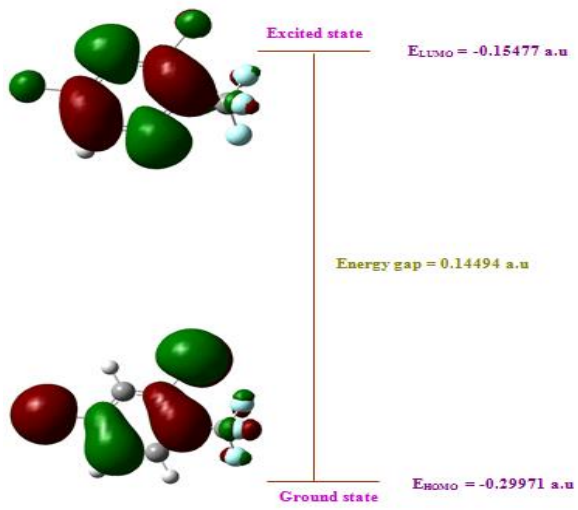

Fig 4. HOMO-LUMO structure of 2,4-dichloro-ααα-trifluorotoluene

Table 1. Optimized geometrical parameters of 2,4-dichloro-ααα-trifluorotoluene computed at LSDA/6-311++G(d,p), B3LYP/6-311++G(d,p) methods and basis set

Bond lengths	Values (Å)		Experimental value[a]	Bond angles	Values (°)		Experimental value[a]	Dihedral angles	Values (°)	
	LSDA	B3LYP			LSDA	B3LYP			LSDA	B3LYP
	6-311++G(d,p)	6-311++G(d,p)			6-311++G(d,p)	6-311++G(d,p)			6-311++G(d,p)	6-311++G(d,p)
C1-C2	1.384	1.389	1.382	C4-C3-C2	118.52	118.57	119.2	C6-C1-C2-C3	-0.0051	0.0017
C1-C6	1.385	1.394	1.380	C4-C3-H12	120.44	120.75	120.8	C6-C5-C4-Cl13	-180	-179.9974
C1-C7	1.089	1.079	1.081	C2-C3-H12	121.04	120.68	120.8	H14-C5-C4-Cl13	179.9955	-179.9992
C2-C3	1.384	1.391	1.377	C1-C2-C3	121.60	121.80	121.3	C2-C1-C6-C5	-0.0035	-0.0013
C2-Cl11	1.787	1.817	1.781	C3-C4-Cl13	119.30	119.33	-	C4-C5-C6-H15	-179.9959	179.9979
C3-C4	1.383	1.391	1.370	C5-C4-Cl13	118.89	118.87	-	H14-C5-C6-C1	179.9959	179.9996
C3-H12	1.089	1.078	1.078	C6-C1-C2	118.50	118.50	119.3	H14-C5-C6-H15	0.0035	-0.0012
C4-C5	1.393	1.402	1.375	C4-C5-H14	121.11	121.12	120.0	C1-C2-C3-C4	0.004	0.0001
C4-Cl13	1.783	1.815	1.774	C6-C5-H14	120.39	120.37	120.4	C5-C4-C3-H12	-179.9893	-179.9998
C5-C6	1.393	1.403	1.375	C3-C4-C5	121.18	121.30	120.2	Cl13-C4-C3-C2	179.9989	179.9992
C5-H14	1.475	1.496	1.469	C3-C2-Cl11	117.73	116.87	-	Cl13-C4-C3-H12	0.0057	-0.0006
C6-H15	1.475	1.496	1.469	C1-C2-Cl11	121.09	121.84	-	C2-C3-C4-C5	0.0057	-0.0023
C7-F8	1.387	1.401	1.375	C4-C5-C6	120.76	121.84	120.1	C4-C3-C2-Cl11	-179.9711	179.9999
C7 - F9	1.387	1.401	1.375	C6-C1-C7	121.90	122.27	121.3	H12-C3-C2-C1	-180.001	179.9975
C7 - F10	1.390	1.401	1.375	C2-C1-C7	119.34	119.22	120.4	H12-C3-C2-Cl11	0.0222	-0.0003
				C1-C6-C5	121.03	121.11	120.2	C3-C2-C1-C6	-0.0139	0.0028
				C1-C6-H15	120.55	119.69	119.8	C3-C2-C1-C7	-179.9824	-179.9908
				C5-C6-H15	119.62	119.19	118.5	Cl11-C2-C1-C6	179.9621	-179.9996
				C1-C7-F8	112.69	112.94	-	H12-C3-C2-Cl11	-0.0064	0.0068
				C1-C7-F9	112.66	112.94	-	C2-C1-C6-C5	0.0128	-0.0009
				C1-C7-F10	111.31	111.78	-	C2-C1-C6-H15	-179.9946	179.9949
				F9-C7-F8	106.64	106.54	-	C7-C1-C6-C5	179.9821	179.9929
				F9-C7-F10	106.55	106.58	-	C7-C1-C6-H15	-0.0253	-0.0063
				F8-C7-F10	106.56	106.06	-	C2-C1-C7-F8	-60.4024	-60.5245
								C2-C1-C7-F9	60.3288	-60.5245
								C2-C1-C7-F10	179.9584	179.971
								C6-C1-C7-F8	119.6293	119.482
								C6-C1-C7-F9	-119.6396	-119.5307
								C6-C1-C7-F10	-0.0099	-0.0226

For numbering of atom refer Fig. 1

[a] For Ref [22].

Table 2. The observed (FTIR and FT-Raman) and calculated (Unscaled and Scaled) frequencies (cm^{-1}), probable assignments (Characterized by TED) of 2,4-dichloro-α,α,α-trifluorotoluene using LSDA/6-311++G(d,p) and B3LYP/6-311++G(d,p) methods and basis set

Symmetry Species C_1	Observed Frequencies		Calculated Frequencies		Scaled Frequencies		Assignments with TED (%)
	FTIR	FT-Raman	LSDA	B3LYP	LSDA	B3LYP	
			6-311++G(d,p)	6-311++G(d,p)	6-311++G(d,p)	6-311++G(d,p)	
A	3111		3156	3227	3114	3112	νCH (100)
A	3099		3151	3225	3103	3102	νCH(100)
A		3095	3140	3210	3096	3095	νCH (99)
A	1600		1628	1624	1590	1591	νC=C (99)
A	1576		1601	1598	1578	1566	νC=C (98)
A	1568		1490	1514	1557	1569	νC=C (98)
A	1390		1411	1416	1380	1381	νCC (95)
A	1332		1392	1326	1320	1324	νCC(89), bCH(10)
A		1319	1319	1320	1319	1311	νCC(89), bCH(9)
A	1295		1249	1286	1282	1283	νCC(80), bCCl(12), bCH(6)
A	1273		1162	1192	1261	1263	CF_3ss (74), bCC(11), bCH(11)
A	1254		1119	1116	1242	1244	CF_3ops (72), CF_3ips(20)
A	1180		1089	1096	1168	1171	bCH (68), bCC(14)
A	1148		1087	1048	1152	1149	bCH(72), Rsymd(13)
A		1230	1073	1045	1219	1221	CF_3ass(59), bCH(18), Rtrigd(11)
A		1117	1013	1020	1122	1120	Rsymd(78), νCC(20)
A	1108		959	997	1098	1099	bCH(60), νCC(22)
A	1083		848	910	1078	1080	Rasymd(92), bCC(6)
A	1039		821	859	1022	1024	Rtrigd(84), bCH(15)
A	1028		802	799	1015	1018	tRtrigd(74), bCC(23)
A	963		706	760	949	950	ωCH(76), νCC(12), bCC(11)
A	871		699	698	868	869	ωCH(70), bCCl(10)
A		832	664	662	816	819	tRsymd(88), ωCC(11)
A	819		587	607	807	809	ωCH(70), ωCC(18)
A		748	559	554	739	740	νCCl(80), bCC(18)
A	733		509	521	724	726	bCC(76), bCH(12)
A		679	504	498	668	669	νCCl(78), bCC(15)
A	667		441	451	654	657	CF_3sb(74), CF_3ips(20)
A	655		431	429	641	642	tRasymd bCH(14)
A	603		390	388	589	591	CF_3 ipb(69), CF_3opb(18)
A	528		374	383	512	516	CF_3 opb(55), CF_3opr(24)
A	457		307	305	442	445	CF_3 ipr(58), ωCC(14), tRtrig((13)
A		409	270	269	396	399	ωCC(80), tRtrigd(23)
A		351	199	211	337	341	CF_3opr(75), tRtrig(24)
A		323	188	187	309	310	bCCl(88), Rsymd(10)
A		282	162	167	268	269	bCCl(80), Rsymd(12)
A		218	153	155	208	210	ωCCl(62), ωCC(16)
A		205	75	75	192	193	ωCCl 60), tRsymd(26)
A		185	52	50	173	175	CF_3 twist(78), ωCC(12)

Abbreviations: ν - stretching; b - in-plane bending; ω - out-of-plane bending; asymd - asymmetric; symd - symmetric; t - torsion; trig - trigonal; ss - symmetric stretching; ass - asymmetric stretching; ips - in-plane stretching,; ops - out-of-plane stretching; sb - symmetric bending; ipr - in-plane rocking; opr - out-of-plane rocking; opb - out-of-plane bending.[a]

Table 3. Second order perturbation theory analysis of Fock matrix in NBO basis corresponding to the intramolecular bonds of 2,4-dichloro-ααα-trifluorotoluene

Donor (i)	Type	ED/e	Acceptor (i)	Type	ED/e	[a]E(2) (kJ mol-1)	[b]E(j) – E(i)	[c]F(i, j) a.u
C1-C2	π	0.84181	C3-C4	π*	0.19071	9.72	0.29	0.068
C1-C2	π	0.84181	C5-C6	π*	0.15664	9.84	0.30	0.069
C3-C4	π	0.83439	C1-C2	π*	0.21824	9.92	0.28	0.068
C3-C4	π	0.83439	C5-C6	π*	0.15664	9.48	0.30	0.067
C5-C6	π	0.82413	C1-C2	π*	21824	11.14	0.26	0.069
C5-C6	π	0.82413	C3-C4	π*	0.19071	11.04	0.26	0.068
F8	n_3	0.96815	C7-F9	σ*	0.04633	5.99	0.60	0.076
F8	n_3	0.96815	C7-F10	σ*	0.04978	5.72	0.61	0.075
F9	n_3	0.96980	C7-F8	σ*	0.04975	5.71	0.61	0.075
F9	n_3	0.96980	C7-F10	σ*	0.04978	5.70	0.61	0.075
F10	n_3	0.96815	C7-F8	σ*	0.04975	5.72	0.61	0.075
F10	n_3	0.96815	C7-F9	σ*	0.04633	5.97	0.60	0.076
Cl11	n_3	0.95967	C1-C2	π*	0.21824	7.06	0.30	0.064
Cl13	n_3	0.96131	C3-C4	π*	0.19071	6.63	0.31	0.062
C1-C2	π*	0.21824	C5-C6	π*	0.15664	80.72	0.02	0.084
C3-C4	π*	0.19071	C5-C6	π*	0.15664	81.83	0.02	0.079

[a] $E^{(2)}$ means energy of hyperconjugative interactions (stabilization energy).
[b] Energy difference between donor and acceptor i and j NBO orbital.
[c] F (i,j) is the Fock matrix element between i and j NBO orbital.

The HOMO-LUMO energy gap of DαααTFT is calculated at B3LYP/6-311++G(d,p) level, which reveals that the energy gap reflects the chemical activity of the compound. The LUMO as an electron acceptor (EA) represents the ability to obtain an electron and HOMO represents ability to donate an electron (ED).

The strong charge transfer interaction through π-conjugated bridge results in substantial ground state donor-acceptor (DA) mixing and the appearance of a charge transfer band in the electron absorption spectrum.

HOMO energy = -0.29971 a.u
LUMO energy = -0.15477 a.u
HOMO-LUMO energy gap = 0.14494 a.u.

The calculated self consistent field (SCF) energy of DαααTFT is -1488.529710 a.u. at B3LYP/6-311++G(d,p). The HOMO and LUMO energy gap explains the fact that eventual charge transfer interaction is taking place within the molecule.

First Hyperpolarizability

The first hyperpolarizability (β) of this novel molecular system and the related properties (β, α_0, Δα) of DαααTFT are calculated using the LSDA and B3LYP method with 6-311++G(d,p) basis set, based on the finite field approach. In the presence of an applied electric field, the energy of a system is a function of the electric field. The first hyperpolarizability is a third-rank tensor that can be described by a 3 × 3 × 3 matrix [48] It can be given in the lower tetrahedral format. It is obvious that the lower part of the 3 × 3 × 3 matrixes is tetrahedral. The components of β are defined as the coefficients in the Taylor series expansion of the energy in the external electric field. When the external electric field is weak and homogeneous, this expansion becomes,

$$E = E^0 - \mu_\alpha F_\alpha - \frac{1}{2}\alpha_{\alpha\beta}F_\alpha F_\beta - \frac{1}{6}\beta_{\alpha\beta\gamma}F_\alpha F_\beta F_\gamma + \ldots \quad (2)$$

Where E^0 is the energy of the unperturbed molecules, F_α is the field at the origin and μ_α, $\alpha_{\alpha\beta}$ and $\beta_{\alpha\beta\gamma}$ are the components of dipole moment, polarizability and the first hyperpolarizabilities, respectively. The total static dipole moment μ, the mean polarizability α_0, the anisotropy of the polarizability Δα and the mean first polarizability β, using the x, y, z components are defined as follows;

$$\mu = \left(\mu_x^2 + \mu_y^2 + \mu_z^2\right)^{\frac{1}{2}}$$

$$\alpha_0 = \frac{\left(\alpha_{xx} + \alpha_{yy} + \alpha_{zz}\right)}{3}$$

$$\Delta\alpha = 2^{\frac{-1}{2}}\left[\left(\alpha_{xx} - \alpha_{yy}\right)^2 + \left(\alpha_{yy} - \alpha_{zz}\right)^2 + \left(\alpha_{zz} - \alpha_{xx}\right)^2 + 6\alpha^2\,xx\right]^{\frac{1}{2}}$$

$$\beta = \left(\beta_x^2 + \beta_y^2 + \beta_z^2\right)^{\frac{1}{2}}$$

and

$\beta_x = \beta_{xxx} + \beta_{xyy} + \beta_{xzz}$
$\beta_y = \beta_{yyy} + \beta_{xxy} + \beta_{yzz}$
$\beta_z = \beta_{zzz} + \beta_{xxz} + \beta_{yyz.}$

The LSDA/6-311++G(d,p) calculated the total molecular dipole moment (μ) and mean first hyperpolarizability (β) are given directly here, 2.7932 Debye and 2.8289×10^{-30} esu respectively, and B3LYP/6-311++G(d,p) calculated, the total molecular dipole moment (μ) and mean first hyperpolarizability (β) are given directly here, 2.9243 Debye and 2.0924×10^{-30} esu respectively which are comparable with the reported values of similar derivatives [49,50]. The large value of hyperpolarizability (β) which is a measure of the non-linear optical activity of the molecular system is associated with the intermolecular charge transfer, resulting from the electron cloud movement through π conjugated frame work from electron donor to electron acceptor groups. So this molecule is an attractive object for future studies of non linear optical properties.

Conclusion

Complete vibrational analysis has been made in the present investigation for proper frequency assignments for 2,4-dichloro-α,α,α-trifluorotoluene. The equilibrium geometries, vibrational frequencies are calculated and analyzed by DFT (LSDA, B3LYP) level of theory utilizing 6-311++G(d,p) basis set. In this study NBO analysis, HOMO and LUMO analysis, first hyperpolarazability, in the 2,4-dichloro-α,α,α-

trifluorotoluene are also discussed elaborately.

References

1 L. Henry, E.R. Yale, Squibb and Sons Inc., US 3, 935, 230 (1976); Appl. 71 (1970) 234.

2 Guenther Grethe, Thomas Mitt, F. Haffman – La Roche and Co., Gen. offen. 2, 806, 909 (1978); Appl. 769 (1977) 816.

3 Russel steiner, Compton and knowier Corp., US 4, 234, 481 (1980); Appl. 847 (1977) 892.

4 Albert J. Clinton, O.K. George O' D'oherty, C. Lilly, Dli and Cor., Us 4, 316, 988 (1982); Appl. 706 (1976) 23.

5 Richo Co., Ltd., Jpn. Knokai Tokkyo Koho Jp 58, 201, 755 (1983); Appl. 82/81 (1982) 570.

6 A. Buzzati – Traverso, Pavia, (iItaly) Farmaco, Ed., Prat., 215 (1986).

7 Max. M. Boudakian, Olin corp., Us 4, 582, 925 (1986); Appl 685 (1984) 6.

8 Edward W. Kluger, Patrick D. Moore, Joe T. Burchette, Milliken Research Corp., Us 4, 761, 502 (1988); Appl. 904 (1986) 459.

9 Miroslav Czech. Veverka (1992); Appl. 88/4 (1988) 496.

10 L. Conte, M. Napoli, G.P. Gambaretto, F.M. Carlini, D. Bonini, J. Fluorine chem., 87 (1998) 19.

11 T. Aoba, crit, Rev. Oral Med. 8(2), (1997) 136.

12 T. Aoba, O. Fejerskov, Crit, Rev. Oval Biol. Med 13(2), (2002) 155.

13 O. Fejerskov, M.J. Larsen, A. Richards, V. Baelum, Adv., Dent., Res., 8(1) (1994) 15.

14 R.G. Parr, W. Yang, Density Functional Theory of Atoms and Molecules, Oxford University Press, New York, 1989

15 S. Sadhukhan, D. Munoz, C. Adamo, G.E. Scuseria, Chem., Phys., Lett. 306 (1999) 83.

16 I.S. Lim, G.E. Scuseria, Chem., Phys., Lett. 460(2008) 137.

17 T. Cai, H. Han, Y. Yua, T. Gao, J. Du. L. Hao., physica B 404(2009) 89.

18 Z. Zhengyu, Du. Dongmei, J. Mol. Struct. (Theochem.) 505(2000) 247.

19 Z. Zhengyu, Fu. Aiping, Du. Dongmei, Int. Quant. Chem., 78(2000) 186.

20 M.J. Frisch, G.W. Trucks, H.B. Schlegal, G.E. Scuseria, M.A. Robb, J.R. Cheesman, G. Zakrzewski, J.A. Montgomerg, Jr., R.E. Stratmann, J.C. Burant, S. Dapprich, J.M. Illam, A.D. Daniels, K.N. Kudin, M.C. Strain, O. Farkas, J. Tomasi, V. Barone, M. Cossi, R. Cammi, B. Mennucci, C. Pomelli, C. Adamo, S. Clifford, J. Ochterski, G.A. Petersson, P.Y. Ayala, Q. Cui, K. Morokuma, N. Rega, P. Salvador, J.J. Dannenberg, D.K. Malich, A.D. Rabuck, K. Raghavachari, J.B. Foresman, J. Cioslowski,J.V. Ortiz, A.G. Baboul, B.B. Stetanov, G. Liu, A. Liashenko, P. Piskorz, I. Komaromi, R. Gomperts, R.L. Martin, D.J. Fox, T. Keith, M.A. Al-Laham, C.Y. Peng, A. Nanayakkara, M. Challacombe, P.M.W. Gill, B. Johnson, W. Chen, M.W. Wong, J.L. Andres, C. Gonzalez, M. Head-Gordon, E.S. Replogle, J.A. Pople, GAUSSIAN 09, Revision A 11.4, Gaussian, Inc, Pittsburgh PA, 2009.

21 Frisch, A.B. Nielson, A.J. Holder, GAVSSIVIEW user Manual, Gaussian Inc., Pittsburgh, P.A. 2009.

22 J. Tonannavar, Jayashree Yenagi, Veenasangeeta Sortur, V.B. Jadhav M.V.Kulkarni, Spectro chim. Acta Part A77(2010) 351.

23 M. Elanthiraiyan B. Jayasudha M. Arivazhagan. Spectrochimica Acta Part A: Molecular and Biomolecular Spectroscopy 134 (2015) 543–552

24 M. Arivazhagan J. Senthil kumar . Spectrochimica Acta Part A: Molecular and Biomolecular Spectroscopy 137 (2015) 490–502

25 V. Arjunan S. Thirunarayanan, G. Durga Devi, S. Mohan Spectrochimica Acta Part A: Molecular and Biomolecular Spectroscopy 150 (2015) 641–651

26 V. Krishnakumar, N. Prabavathi, Spectrochimica Acta A 71 (2008) 449 .

27 A. Altun, K. Golcuk, M. Kumru, Journal of Molecular Structure (THOCHEM) 637 (2003) 155.

28 S.J. Singh, S.M. Pandey, Indian Journal of Pure and Applied Physics 12 (1974) 300.

29 Y. – X. Sun, Q – L. Hao, Z – X. Yu, W – J. Jiang, L. – D. Lu, X. Wang, Spectrochimica Acta A 73 (2009) 892.

30 M. Arivazhagan, D. Anitha Rexalin, G. Ilango, Spectrochimica Acta Part A 121 (2014) 641.

31 N. Sundaraganesan, B. Dominic Joshua, T. Rjakumar, Indian Journal of Pure and Applied Physics 47 (2009) 248.

32 R. Gayathri, M. Arivazhagan, Spectrochimica Acta Part A 123(2014)309.

33 P.S. Kalai, Spectroscopy of Organic Compounds, Wiley Eastern Limited, New Delhi 1993, p. 117.

34 A.R. Prabakaran, S. Mohan, Indian Journal of Physics 63B (1989) 468.

35 C.S. Hiremath, T. Sundius, Spectrochimica Acta A 74 (2009) 1260.

36 M. Arivazhagan, D. Anitha Rexalin Spectrochemica, Acta Part A 130 (2014) 502.

37 G. Varsanyi, Assignments for Vibrational Spectra of 700 Benzene Derivatives Vol. 1. Hilger, London, 1974.

38 L.E. Fernandez, A. Benaltabef, A. Navarro, M. Fernandez Gomez, E.L. Varetti, Spectrochim Acta 56 A (2000) 1101.

39 L.E. Fernandez, A. Ben Altabet, E.L.Varetti, J. Mol. Structure 612 (2002).

40 T.K. Gounev, Gamil, A.Guirgis, James R. Durig, J. Mol. Struct. 436-437 (1997) 613.

41 M.E. Tuttolomondo, L.E. Fernandez, A. Navarro, E.L. Varett, A. Benaltabef, spectrochim Acta 60A (2004) 611.

42 D. Aruldhas, I. Hubert Joe, S.D.D.Roy, T.H. Freeda, Spectrochimica Acta Part A77 (2010) 36.

43 E.D. Glendening, J.K. Badenhoop, A.E. Reed, J.E. Carpenter, J.A. Bohmann, C.M. Morales, F. Weinhold, NBO 5.0, Theoretical chemistry Institute, University of Wisconsin, Madison, 2001.

44 T. Vijayakumar, I.H. Joe, V.S. Jayakumar, Chem. phys, 343 (2008) 83.

45 J. Karpagam, N. Sundaraganesan, S. Sebastian, S. Manoharan, M. Kurt, J. Raman Spectrosc. 41(2010) 53.

46 E. Kavitha, N. Sundaraganesan, S. Sebastin, Indian J. Pure Appl. Phys, 48 (2010) 20.

47 O. Prasad, L. Sinha, N. Kumar, J. At. Mol. Sci. 1 (2010) 201.

48 D.A. Klein man, Phys. Rev. 126 (1962) 1977.

49 V.B. Jothy, T. Vijayakumar, V.S. Jayakumar, K. Udayalekshmi, Ramamoorthy I. Hubert Joe, J. Raman Spectrosc. 38 (2007) 1148.

50 Virendra Kumar, Y. Panikar, M.A. Palatox, J.K. Vats, I. Kostova, K. Lang, V.K. Rastogi, Indian J. Pure Appl. Phys. 48 (2010) 85-94.